THE SPECTROSCOPIC BINARY η ANDROMEDAE: DETERMINATION OF THE ORBIT BY OPTICAL INTERFEROMETRY

C.A. HUMMEL[1], J.T. ARMSTRONG[1], A. QUIRRENBACH[1], D.F. BUSCHER[1], D. MOZURKEWICH[2], R.S. SIMON[2], AND K.J. JOHNSTON[2]

NRL/USNO Optical Interferometer Project

U.S. Naval Observatory, 3450 Massachusetts Avenue NW, Washington, DC 20392

[1]Universities Space Research Association, 300 D St. SW, Suite 801, Washington, DC 20024

[2]Remote Sensing Division, Naval Research Laboratory, Code 7200, Washington, DC 20375

ABSTRACT

We have determined the following orbital elements of the double-lined spectroscopic binary η Andromedae (combined spectral class G8IIIb) using measurements with the Mark III long baseline optical interferometer on Mt. Wilson: period $P = 115.72 \pm 0.02$ d, major axis $a = 10.37 \pm 0.03$ milliarcseconds, eccentricity $e = 0.006 \pm 0.002$, epoch of periastron $T = \mathrm{JD}2448013 \pm 2$, inclination $i = 30\overset{\circ}{.}5 \pm 0\overset{\circ}{.}4$, argument of ascending node $\Omega = 69\overset{\circ}{.}4 \pm 0\overset{\circ}{.}6$, and argument of periastron $\omega = 215^\circ \pm 7^\circ$. The magnitude differences of the two components measured at $\lambda\lambda$ 800 nm, 550 nm, and 500 nm are $0\overset{\mathrm{m}}{.}50 \pm 0\overset{\mathrm{m}}{.}06$, $0\overset{\mathrm{m}}{.}55 \pm 0\overset{\mathrm{m}}{.}08$, and $0\overset{\mathrm{m}}{.}56 \pm 0\overset{\mathrm{m}}{.}09$, respectively. Using orbital elements from spectroscopy by Gordon (1946) we derive component masses of (2.59 ± 0.30) $\mathrm{M}_\odot$ and (2.34 ± 0.22) $\mathrm{M}_\odot$, and a distance of (76 ± 2) pc. Monte-Carlo simulations have been performed to estimate parameter uncertainties. We discuss the evolutionary state of η Andromedae.

1. INTRODUCTION

Observations using long baseline optical interferometry have the potential to resolve a large fraction of the known spectroscopic binaries, thus providing us with the possibility of determining masses, distances and luminosities for many more stars among the double-lined systems (Armstrong *et al.* 1992a, 1992b; Pan *et al.* 1990). In 1989, we selected 255 stars brighter than fifth magnitude in the V band and north of $-10°$ declination from the catalog of Batten, Fletcher, & MacCarthy (1989) and from other lists. Observations were carried out using the Mark III optical interferometer[3] at wavelengths of 800 nm, 550 nm, and 500 nm (450 nm in 1989) on baselines ranging from 3 m to 31 m in length (3 milliarcseconds [mas] maximum resolution). The interferometer has been described by Shao *et al.* (1988) and Mozurkewich *et al.* (1991). As of 1992, we have found significant nightly visibility variations, indicative of multiplicity, for half of the ≈80 systems which have a sufficient amount of data. 24 orbits have been determined, with major axes ranging from 3.4 mas to 124 mas. The largest magnitude difference between the two binary components measured is about $3^{\rm m}$ (the larger the magnitude difference, the smaller the visibility variations).

The star η Andromedae (= 38 And = HR 271 = HD 5516 = SAO 74388 = Batten 50, $\alpha = 0^{\rm h}57^{\rm m}12.4^{\rm s}$, $\delta = 23°25'04''$ [epoch 2000.0], $m_V = 4\overset{\rm m}{.}42$) was found to be a spectroscopic binary, with the spectra of both components visible, by Campbell and Wright (1900). Gordon (1946) obtained fifty spectrograms at Lick Observatory and derived the elements for the spectroscopic orbit listed in Table 1. The spectra were consistently classified as those of two similar G8III-IV components (e.g. Roman 1952). The star was listed as a probable member of the Ursa Major stream (Roman 1949). η Andromedae is very similar to

---

[3]The Mark III Optical Interferometer located on Mt. Wilson near Los Angeles, California, is operated by the Remote Sensing Division of the Naval Research Laboratory (NRL) with funding from the Office of Naval Research.

the double-lined spectroscopic binary ϕ Cygni (regarding spectral types, colors, magnitude difference, and masses of the components), for which an interferometric orbit has been determined recently (Armstrong *et al.* 1992b).

2. OBSERVATIONS

The data were obtained during 23 nights in summer and autumn of 1990, 1991 and 1992 (mean epoch JD 2448307 = 1991.1). We measured the stellar fringe visibility in three channels, centered at $\lambda\lambda$ 800 nm, 550 nm, and 500 nm (22 nm, 25 nm, and 25 nm bandwidth, respectively), on the north-south baselines of the Mark III interferometer with lengths ranging from 12.0 m to 31.5 m. In a typical night on a given baseline, 15 scans of 75 seconds on-source duration were recorded, with an equal number of scans on a nearby calibrator star. After each scan, a background measurement was taken. The observations were switched with other program and calibrator stars during the night. The calibrator stars are chosen to have small angular diameters, so that the visibility measured by an ideal interferometer would be close to unity. Their diameters were estimated from their apparent visual magnitude and the $(R - I)$ color index using a procedure given by Mozurkewich *et al.* (1991).

The Mark III interferometer tracks the rapid fringe motion (induced by atmospheric turbulence) in a broadband channel (650 nm – 900 nm) and coherently averages the fringe pattern in each of the four channels for 4 ms. The square of the visibility amplitude, V^2, is calculated off-line and integrated incoherently to 0.5 seconds. Only data from the narrow channels are used for further analysis, since the visibility amplitude degradation when the Mark III tracks one or two fringes off the central fringe is negligible for these small bandwidths.

The visibility amplitudes were corrected for the background count, edited and further

averaged over the duration of the scan. The calibration of the data follows the procedures described in detail by Armstrong *et al.* (1992a) and Mozurkewich *et al.* (1991). Essentially, the amplitudes are normalized by the ratio of measured to estimated amplitudes for the calibration stars. The normalization factor is a function of the seeing index, zenith angle, siderostat mirror angle and time (the seeing dependence usually being the strongest). Estimates for the uncertainties of the visibility amplitudes are calculated as the square root of the sum of the statistical variance of the 0.5 s averages and the square of the calibration uncertainty. The latter is defined as the uncertainty which, when added to the statistical variance in quadrature, results in a reduced χ^2, χ^2_ν, of unity for the fit of the calibrator amplitudes to their estimated values.

3. DETERMINATION OF THE ORBIT

The visibility amplitudes of the binary measured with the Mark III interferometer as a function of time during the night are fully represented by a model with eleven parameters. These include the separation ρ and position angle θ (if changes due to orbital motion are negligible), plus nine system parameters: two uniform disk diameters $D_{1,2}(\lambda)$ and a magnitude difference $\Delta m(\lambda)$ at the three narrow-band channel center wavelengths. The ρ and θ are functions of time and of the seven orbital elements, i.e. the major axis a in mas, eccentricity e, period P, epoch of periastron passage T, inclination i, argument of the ascending node Ω, and the argument of the periastron ω. If the components of the binary are non-variable, the binary system thus is completely represented by a total of sixteen parameters. We point out that, since we are not able to measure the visibility phase, the identity of the components can not be determined, i.e. ω is ambiguous by 180°.

We used the method described by Armstrong *et al.* (1992b) to fit ρ and θ to the visibility variations due to the changing baseline orientation during the night. We used the Thiele-Innes method to obtain an initial estimate of the orbital parameters from these (ρ,

θ) pairs. Using this initial estimate, we then performed a non-linear least squares fit of all seven orbital elements and five system parameters to the data (Levenberg-Marquardt method: Press *et al.* 1992). We adopted $D_{1,2}(\lambda)/D_{1,2}(800\text{nm}) = 0.95$ for $\lambda = 500$ nm and $\lambda = 550$ nm due to limb darkening (see Mozurkewich *et al.* 1991). The advantages of this procedure are its use of all data to constrain the system parameters (rather than the calculation of a mean from the results of individual nights), its ability to derive orbital elements if the orbital motion during a night is not negligible, and its use of nights with an amount of data insufficient to constrain a fit of ρ and θ. The results are listed in Table 2. The reduced χ^2_ν of the fit is 1.05 (966 visibility measurements). Comparing our results for e and P with the spectroscopic results from Gordon (1946), we find agreement within the uncertainties.

The orbit is shown in Fig. 1. In the figure, a little arrow indicates the sense of revolution, and the letter T denotes the periastron. Binary positions and corresponding uncertainty ellipses were derived from the data of each night in order to indicate the amount and quality of the data and their weight in constraining the orbital fit. Figure 2 presents enlargements of selected areas of Fig. 1. The uncertainty ellipses were calculated as follows: we adopted the diameters and magnitude differences from the global fit (see Table 2) and determined a value for separation and position angle of the binary from the data for each night. The visibility uncertainties were scaled to normalize the reduced χ^2_ν of the fit to unity, and an uncertainty ellipse was defined as the boundary of (ρ,θ) values leading to an increase of the total χ^2 by one.

Table 3 lists the results; cols. 1 and 2 give date and fractional Besselian year of the observation, col. 3 the length of the baseline used, col. 4 the number of scans obtained, cols. 5 and 6 separation and position angle of the binary, cols. 7 to 9 the axes and the position angle of the uncertainty ellipse, and col. 10 the deviation of the fitted binary position from

the model values for ρ and θ.

4. ESTIMATION OF PARAMETER UNCERTAINTIES

The formal uncertainties derived from the diagonal elements of the covariance matrix (the inverse of which is used in the Levenberg-Marquardt algorithm to find the minimum of the linearized χ^2-hypersurface) could be underestimates of the true uncertainties for two reasons. The first is the non-linearity of the binary model: if, for instance, $\Delta m = 0\overset{\mathrm{m}}{.}5$, an uncertainty in the squared minimum visibility, $V^2_{\rm min}$, of $0\overset{\mathrm{m}}{.}05$ makes Δm consistent with zero, while if $\Delta m = 2^{\rm m}$, the same uncertainty in $V^2_{\rm min}$ produces an uncertainty in Δm of about $0\overset{\mathrm{m}}{.}2$. (The maximum and minimum squared visibilities of a binary are $V^2_{\rm max,min} = ((F \pm 1)/(F+1))^2$ for unresolved components, with $F = S_1/S_2$, the ratio of the fluxes of the two components.) The second reason for an underestimate of the uncertainties is the possibility of a non-normal distribution of the visibility errors (i.e. the deviations of the measured visibilities from the model visibilities, divided by the formal uncertainties). Figure 3 shows that the distribution of O-C values for the calibrators is slightly broadened for our data.

In order to get an independent estimate of parameter uncertainties we created synthetic data sets for a Monte Carlo simulation using three different methods.

Method (i) replaces the observed data with the model visibilities, adds visibility errors with a normal distribution of $\sigma = 1$ and applies artificial calibration errors generated by the following procedure. For each night and channel, (absolute) calibration errors for each calibrator were smoothed with a two-hour $1/e$ timescale and extrapolated to the same observing interval using linear prediction (Press *et al.* 1992). Power spectra of the calibration errors were then calculated, averaged over all calibrators of that night, and transformed back with random phases to simulate random errors in the calibration.

The same random phases were used for all channels, since calibration errors are usually correlated between channels due to common origins in siderostat drive errors, changes in the seeing characteristics and instrumental drifts.

Method (ii) applies an additional final calibration to the binary visibilities of each night using smoothed absolute errors of a single calibrator, which is selected on a random basis from any night ("calibrator shuffling").

Method (iii) is the "bootstrap" method as descibed by Press *et al.* (1992) and works as follows. A copy of the original data set is made, from which one record after another is selected on a random basis, each time replacing the "removed" record by a record from the original data set (again on a random basis). This procedure is repeated N times for a set of N original records.

Some 300 sets of data were simulated with each of the three methods and the distribution of the binary parameters fitted to the data determined. For all three methods and all parameters, the distributions are roughly Gaussian, with the peak centered on the binary model value (see Table 2). The widths of the distributions are close to values consistent with the formal uncertainties, the power spectrum method giving slightly larger widths usually. In Table 2, we list the parameter ranges spanning the central two-thirds of the fitted parameter values. We see that the formal uncertainties provided a good estimate of the parameter uncertainties.

The Monte-Carlo simulations also allow us to study details of correlations between parameters. (They "visualize" correlations indicated by non-zero off-diagonal elements in the covariance matrix of the parameters.) Figure 4 shows significant correlations between the two stellar diameters, diameters and magnitude differences, the eccentricity and the period, and the major axis and the inclination. (The correlation between the epoch and the argument of periastron, which is expected for a nearly circular orbit, has been omitted.) All

other correlations are insignificant. The meaning of these correlations is that combinations of the parameters (ratios, for example) have larger (or smaller) uncertainties than expected from formal error propagation of independent errors in the single parameters (even though the Monte-Carlo parameter distributions give the correct estimates for the spread in single parameters). The correlation between the two stellar diameters is explained by the fact that due to the small magnitude difference in all channels and the lack of visibility phases, the identity of the components is ill-defined and a larger resolution of one of the components can be offset by a smaller resolution of the other component. The correlation between diameters and magnitude differences arises from the similar effect diameters and magnitude differences have on the amplitude of the nightly visibility variations: the larger they are, the smaller the amplitudes. The correlation between the eccentricity and the period is related to the fact that both parameters determine the rate of orbital motion. Finally, the correlation between the major axis and the inclination is due to the projection effect with varying inclination.

5. DISCUSSION

5.1 Absolute magnitudes, colors, and diameters

Using the values for $K_{1,2}$, P, a, e and i, we derived a distance of (76.2 ± 1.8) pc to η Andromedae (orbital parallax $= 0\farcs0131 \pm 0\farcs0003$, distance modulus $= -4\fm41 \pm 0\fm05$). For giants of spectral class G8 we expect $(B-V) = 0\fm94$ and $(U-B) = 0\fm70$ (Schmidt-Kaler 1982). Comparing these to the measured values $(B-V) = 0\fm94$ and $(U-B) = 0\fm69$ (Hoffleit & Jaschek 1982) we conclude that interstellar reddening has a negligible effect for our purposes, as expected from the small distance to the system. On the assumption of η Andromedae being a member of the Ursa Major stream, Roman (1949) derived a cluster parallax of $0\farcs014$, in good agreement with our orbital parallax.

With the magnitude differences measured, we calculated (absolute) magnitudes of each component from the combined magnitudes given by Johnson *et al.* (1966) in the $UBVRI$ system and the distance. We extrapolated the magnitude difference to the B-band from our 500 nm band and used the formula given by Bessell (1979) to convert $(V-I_{\rm J})$ to $(V-I_{\rm C})$ (the Cousins I-band at 789 nm is close to our 800 nm band). We adopted (independent) uncertainties in the B, V, and $I_{\rm C}$ bands of $0\fm02$, $0\fm03$, and $0\fm03$, respectively. Table 4 lists the results. We derived $(B-V)$ values of $0\fm93 \pm 0\fm08$ for the primary component and $0\fm95 \pm 0\fm10$ for the secondary.

The mean effective temperature of the components of η Andromedae was derived by McWilliam (1990) to be $\log(T_{\rm eff}/{\rm K}) = 3.69$ (Gottlieb & Bell 1972 give $\log(T_{\rm eff}/{\rm K}) = 3.70$). At this temperature, Gubochkin & Miroshnichenko (1991) determined a bolometric correction of $B.C. = 0\fm32 \pm 0\fm05$. Values given by Allen (1976) and Popper (1980) for this effective temperature agree within the quoted uncertainty, Schmidt-Kaler (1982) gives $B.C. = 0\fm42$. Because of the similarity of the two components, we applied the same $B.C.$

($0\overset{\mathrm{m}}{.}32$) to both absolute visual magnitudes to derive luminosities of $\log(L/L_\odot) = 1.81 \pm 0.02$ for the primary, and $\log(L/L_\odot) = 1.59 \pm 0.03$ for the secondary (using the relation $M_{\rm Bol} = -2.5 \log(L/L_\odot) + 4\overset{\mathrm{m}}{.}72$).

Diameters of the size reported in Table 4 are too small to be measured with high precision with the Mark III interferometer. Blackwell *et al.* (1991) derived a (limb darkened) diameter of 1.63 mas for η Andromedae assuming a single star and using the infrared flux method. Adopting identical colors for the primary and secondary, the V band magnitude difference translates into a diameter ratio of 1.29, and the individual diameters become 1.3 mas and 1.0 mas, respectively. These values are consistent with our diameters (see Table 4).

5.2 Masses and evolutionary state

The determination of the orbital inclination allows us to derive the component masses for η Andromedae using e and Gordon's (1946) values for P and $K_{1,2}$: $2.59 \pm 0.30 \mathcal{M}_\odot$ for the primary, and $2.34 \pm 0.22 \mathcal{M}_\odot$ for the secondary. The uncertainty in the mass determination is largely caused by the uncertainty in $K_{1,2}$. (If the uncertainties were entirely due to the uncertainty of the interferometric orbit, they would decrease by a factor of 2.) Combining the values for component masses, diameters (see the previous paragraph), and the distance to η Andromedae, we derived surface gravities of $\log g = 2.8$ and $\log g = 3.0$ (cgs units) for the primary and secondary, respectively. These values are consistent with those for giants of classes K0 and G8 (Allen 1976). In the following we will compare masses, luminosities, and colors with results of various evolutionary models. Due to the large uncertainties in the masses, however, a more detailed discussion will have to await better spectroscopic measurements.

With the advent of new opacity tables, calculated by Rogers & Iglesias (1992), modified stellar evolution models have been published (e.g. Stothers & Chin 1991, Meynet *et al.*

1993). We used the stellar model grids presented by Schaller *et al.* (1992) and Schaerer *et al.* (1993) for metallicities Z =0.001, 0.008, and 0.020 (the tables of evolutionary tracks as well as a program to construct isochrones kindly were made available to us by G. Meynet). We found a pair of coeval model stars of solar metallicity at log(age/y)=8.9, with masses, colors, and luminosities consistent (within about 1σ) with the results for the components of η Andromedae. These model parameters are, for the primary component: $\mathcal{M} = 2.38\mathcal{M}_{\odot}$, $\log(g) = 2.7$, $\log(L/L_{\odot}) = 1.84$, $\log(T_{\rm eff}/{\rm K}) = 3.69$, $M_{\rm V} = 0\overset{\rm m}{.}47$, and $(B-V) = 0\overset{\rm m}{.}98$, and for the secondary component: $\mathcal{M} = 2.26\mathcal{M}_{\odot}$, $\log(g) = 2.9$, $\log(L/L_{\odot}) = 1.62$, $\log(T_{\rm eff}/{\rm K}) = 3.69$, $M_{\rm V} = 0\overset{\rm m}{.}98$, and $(B-V) = 0\overset{\rm m}{.}94$. This scenario, where only the primary component has already undergone helium ignition, gives a mass ratio of about 1.05 (compare this to $K_2/K_1 = 1.11 \pm 0.07$). We show the corresponding isochrone and the color-magnitude data of η Andromedae in Fig. 5.

There exists a pair of coeval stars of a lower metallicity Z =0.008 at log(age/y)=9.0, providing an even better fit to the color-magnitude data. However, in this model, the masses come out to be too small. From spectroscopic measurements, McWilliam (1990), Gottlieb & Bell (1972), and Hansen & Kjærgaard (1971) have derived values for the metallicity [M/H]= $\log(Z/Z_{\odot})$ of η Andromedae of -0.54, 0.0, and -0.16, respectively. Considering the spread in these values, the adoption of a solar-type metallicity is consistent with the measurements.

We finally turn to the question of the probable membership of η Andromedae in the Ursa Major stream. In 1993, Soderblom & Mayor used the stellar evolution models by VandenBerg (1985) to derive the age of the Ursa Major stream to be $\approx$ 300 million years. They determined a mean metallicity of the stream members of [M/H]= -0.08 ± 0.09. Correlating the lists from McWilliam (1990) and Hansen & Kjærgaard (1971) with the list of probable stream members from Roman (1949), we found the mean metallicity of stream

members to be -0.2 ± 0.2 and -0.3 ± 0.2, respectively (uncertainties encompass almost all metallicity values). Thus, using the new models with metallicity $Z = 0.008$ ([M/H]$= -0.3$), we obtained a reasonable fit to the color-magnitude data of the Ursa Major stream (taken from Soderblom & Mayor 1993) with the isochrone of log(age/y)=8.7 (see Fig. 5). The isochrone for η Andromedae provides a clearly inferior fit to the stream data, so that we have to conclude that this system is probably not a member of the Ursa Major stream. We note that Eggen (1958) excluded η Andromedae from the list of probable stream members based on its space velocity.

6. CONCLUSIONS

We have determined the orbital elements of the double-lined spectroscopic binary η Andromedae and derived masses, luminosities, diameters, and colors of the components, using additional elements provided by spectroscopy (Gordon 1946). Results were compared with the evolutionary models by Schaller *et al.* (1992) and Schaerer *et al.* (1993), and a coeval stellar pair was found with consistent properties. Uncertainties in the spectroscopic elements, however, did not allow a more detailed analysis. With a large number of spectrocopic binaries resolved and orbits determined by long baseline optical interferometry with high precision (Hummel & Armstrong 1993), new spectroscopic measurements become necessary to help remove the limitation of high precision mass determinations to the eclipsing binaries.

We thank Lu Rarogiewicz and Craig Denison for helping operate the Mark III interferometer during long nights of observing for many years. We also thank Georges Meynet for his prompt help regarding the use of the Geneva Observatory stellar evolution models. This work was supported by the Office of Naval Research. A. Q. is supported by

the Alexander von Humboldt foundation through a Feodor Lynen fellowship. This research has made use of the SIMBAD literature database, operated at CDS, Strasbourg, France.

References

Allen, C. W. 1976, Astrophysical Quantities (Athlone Press, London)

Armstrong, J. T., Mozurkewich, D., Vivekanand, M., Simon, R. S., Denison, C. S., Johnston, K. J., Pan, X.-P., Shao, M., & Colavita, M. M. 1992a, AJ, 104, 241

Armstrong, J. T., Hummel, C. A., Quirrenbach, A., Buscher, D. F., Mozurkewich, D., Vivekanand, M., Simon, R. S., Denison, C. S., Johnston, K. J., Pan, X.-P., Shao, M., & Colavita, M. M. 1992b, AJ, 104, 2217

Batten, A. H., Fletcher, J. M., & MacCarthy, D. G. 1989, Pub. Dom. Astrophys. Obs., 17, 1

Bessell, M. S. 1979, PASP, 91, 589

Blackwell, D. E., Lynas-Gray, A. E., & Petford, A. D. 1991, A&A, 245, 567

Campbell, W. W., & Wright, W. H. 1900, ApJ, 12, 256

Eggen, O. J. 1958, MNRAS, 118, 65

Gordon, K. C. 1946, ApJ, 103, 13

Gottlieb, D. M., & Bell, R. A. 1972, A&A, 19, 434

Gubochkin, A. N., Miroshnichenko, A. S. 1991, Kin. and Phys. of Cel. Bodies, 7, 59

Hansen, L., & Kjærgaard, P. 1971, A&A, 15, 123

Hoffleit, D., & Jaschek, C. 1982, The Bright Star Catalogue (Yale University Observatory, New Haven)

Hummel, C. A., & Armstrong, J. T. 1993, Proc. of IAU Symp. 158 (preprint)

Johnson, H. L., Mitchell, R. I., Iriarte, B., & Wiśniewski, W. Z. 1966, Comm. Lunar Planetary Lab., 4, 99

Meynet, G., Mermilliod, J.-C., & Maeder, A. 1993, A&AS, 98, 477

McWilliam, A. 1990, ApJS, 74, 1075

Mozurkewich, D., Johnston, K. J., Simon, R. S., Bowers, P. F., Gaume, R. A., Hutter, D. J., Colavita, M. M., & Shao, M. 1991, AJ, 101, 2207

Pan, X.-P., Shao, M., Colavita, M. M., Mozurkewich, D., Simon, R. S., & Johnston, K. J. 1990, ApJ, 356, 641

Popper, D. M. 1980, ARAA, 18, 115

Press, W. H., Flannery, B. P., Teukolsky, S. A., & Vetterling, W. T. 1992, Numerical Recipes (Cambridge University Press, Cambridge)

Rogers, F. J., & Iglesias, C. A. 1992, ApJS, 79, 507

Roman, N. G. 1949, ApJ, 110, 205

Roman, N. G. 1952, ApJ, 116, 122

Schaller, G., Schaerer, D., Meynet, G., & Maeder, A. 1992, A&AS, 96, 269

Schaerer, D., Meynet, G., Maeder, A., & Schaller, G. 1993, A&AS, 98, 523

Schmidt-Kaler, T. H. 1982, Physical Parameters of the Stars, in: Landolt-Bornstein New Series, Vol. 2b eds. K. Schaifers and H. H. Voigt (Springer Verlag, New York)

Shao, M., Colavita, M. M., Hines, B. E., Staelin, D. H., Hutter, D. J., Johnston, K. J., Mozurkewich, D., Simon, R. S., Hershey, J. L., Hughes, J. A., & Kaplan, G. H. 1988, A&A, 193, 357

Soderblom, D. R., & Mayor, M. 1993, AJ, 105, 226

Stothers, R. B., & Chin, C.-W. 1991, ApJL, 381, L67

VandenBerg, D. A. 1985, ApJS, 58, 711

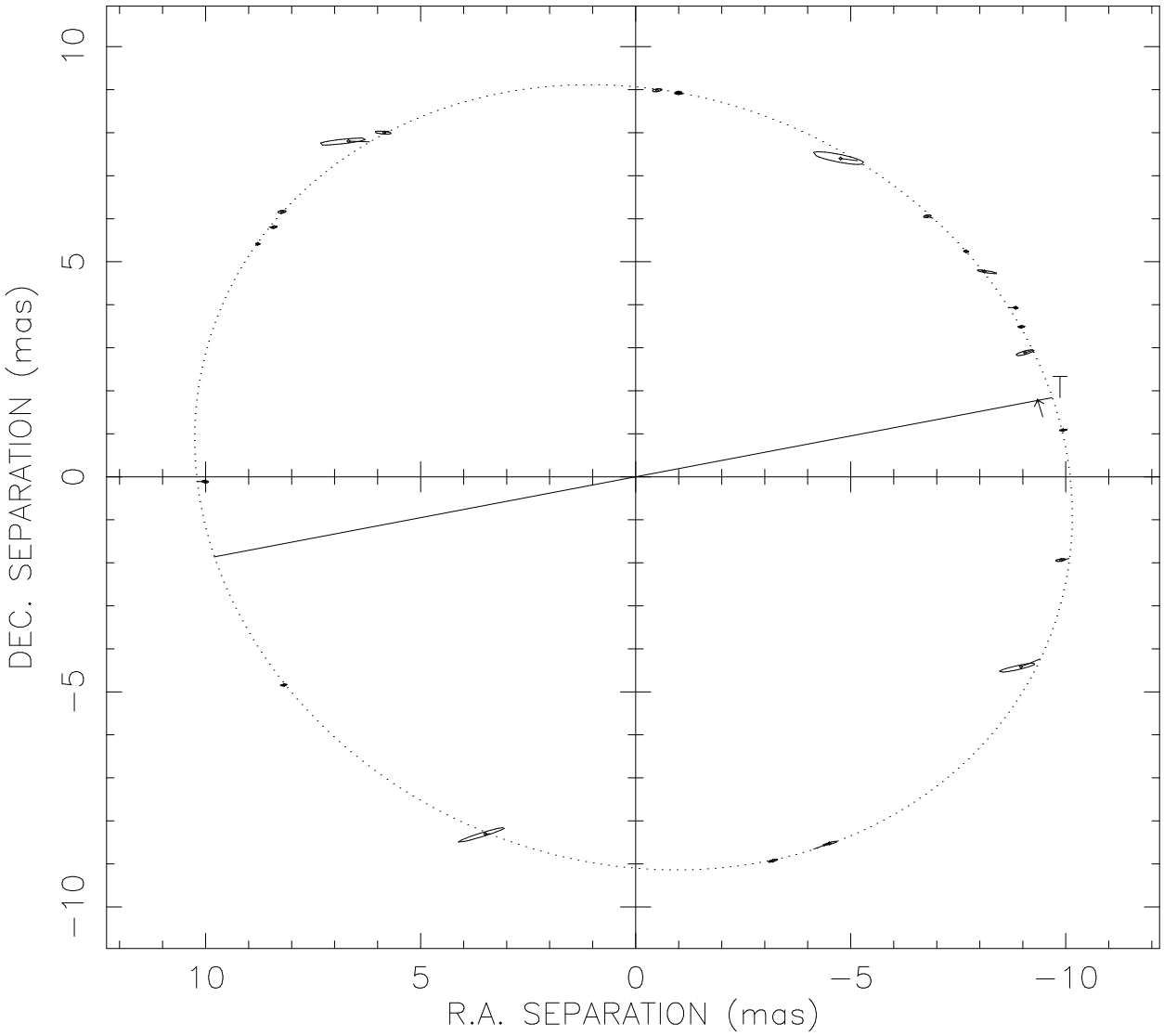

Fig. 1.— The orbit of η Andromedae.

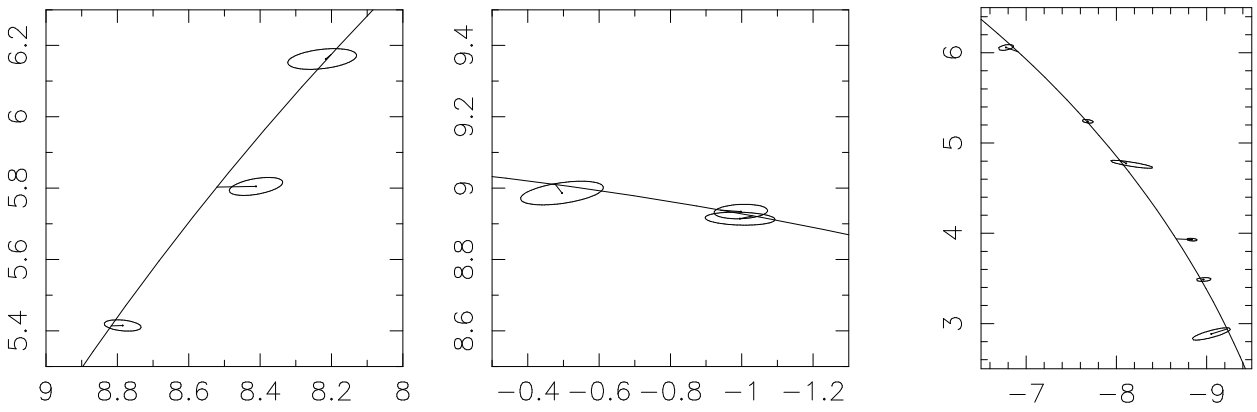

Fig. 2.— Selected areas of the orbit.

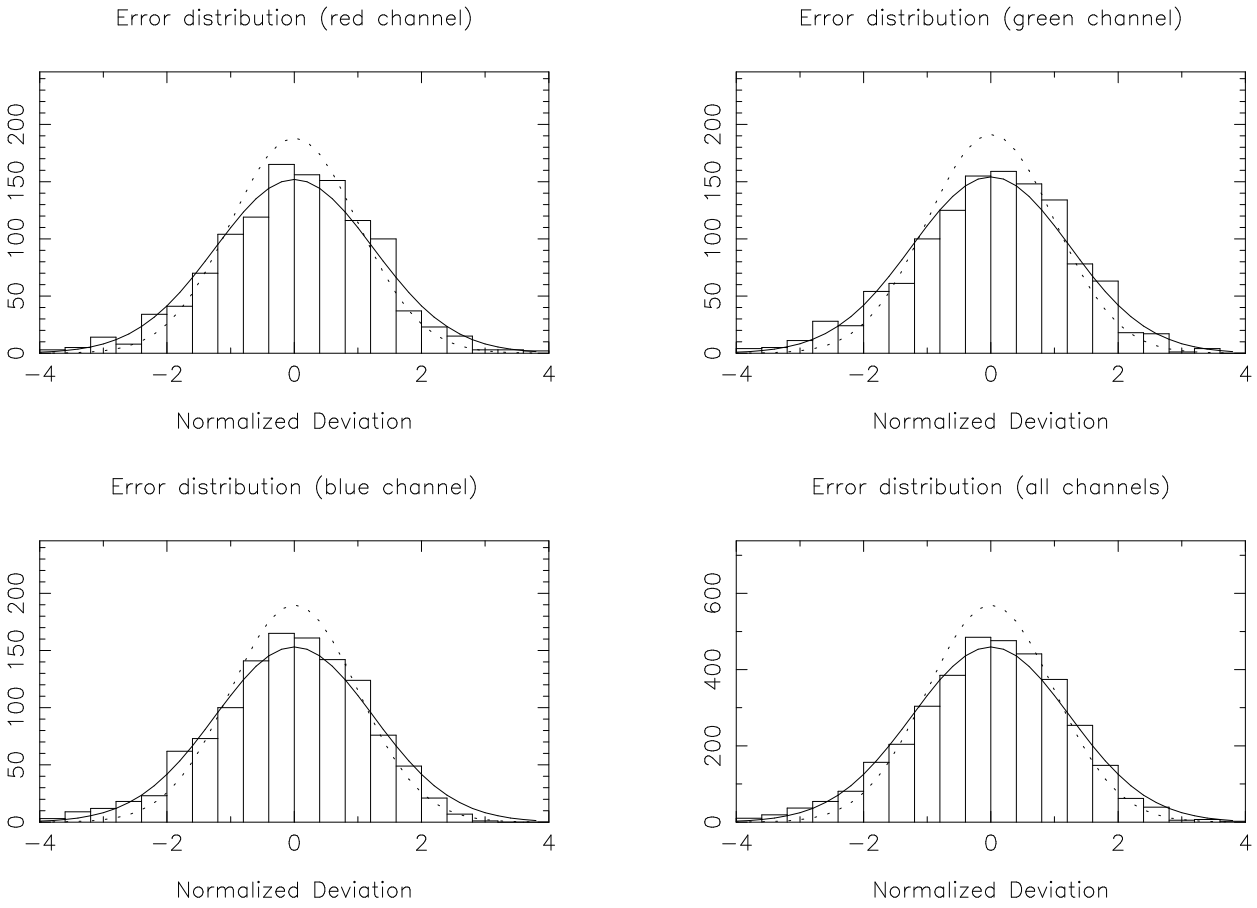

Fig. 3.— Visibility error histograms for the calibrators. The dotted curves are for $\chi^2_\nu = 1.0$, the solid curves for $\chi^2_\nu = 1.5$.

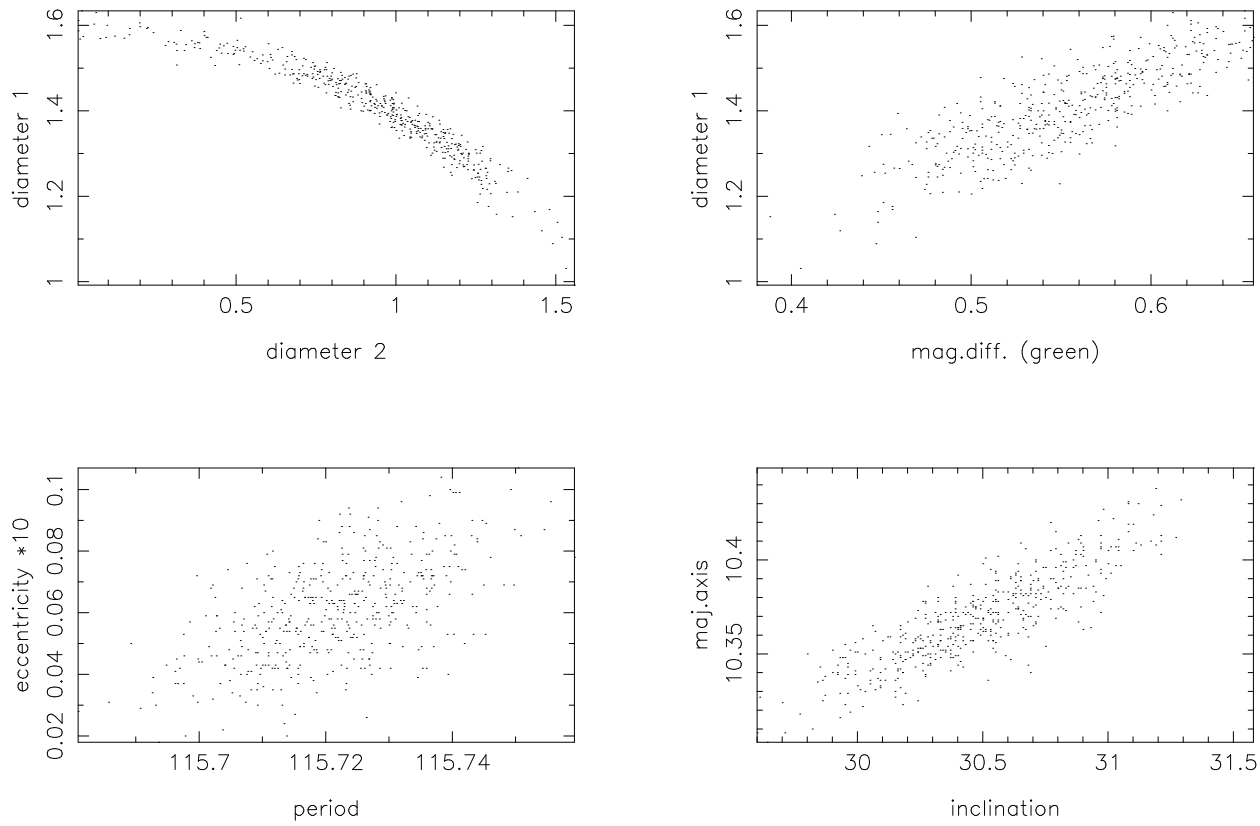

Fig. 4.— Correlation between parameters (units are the same as in Table 2).

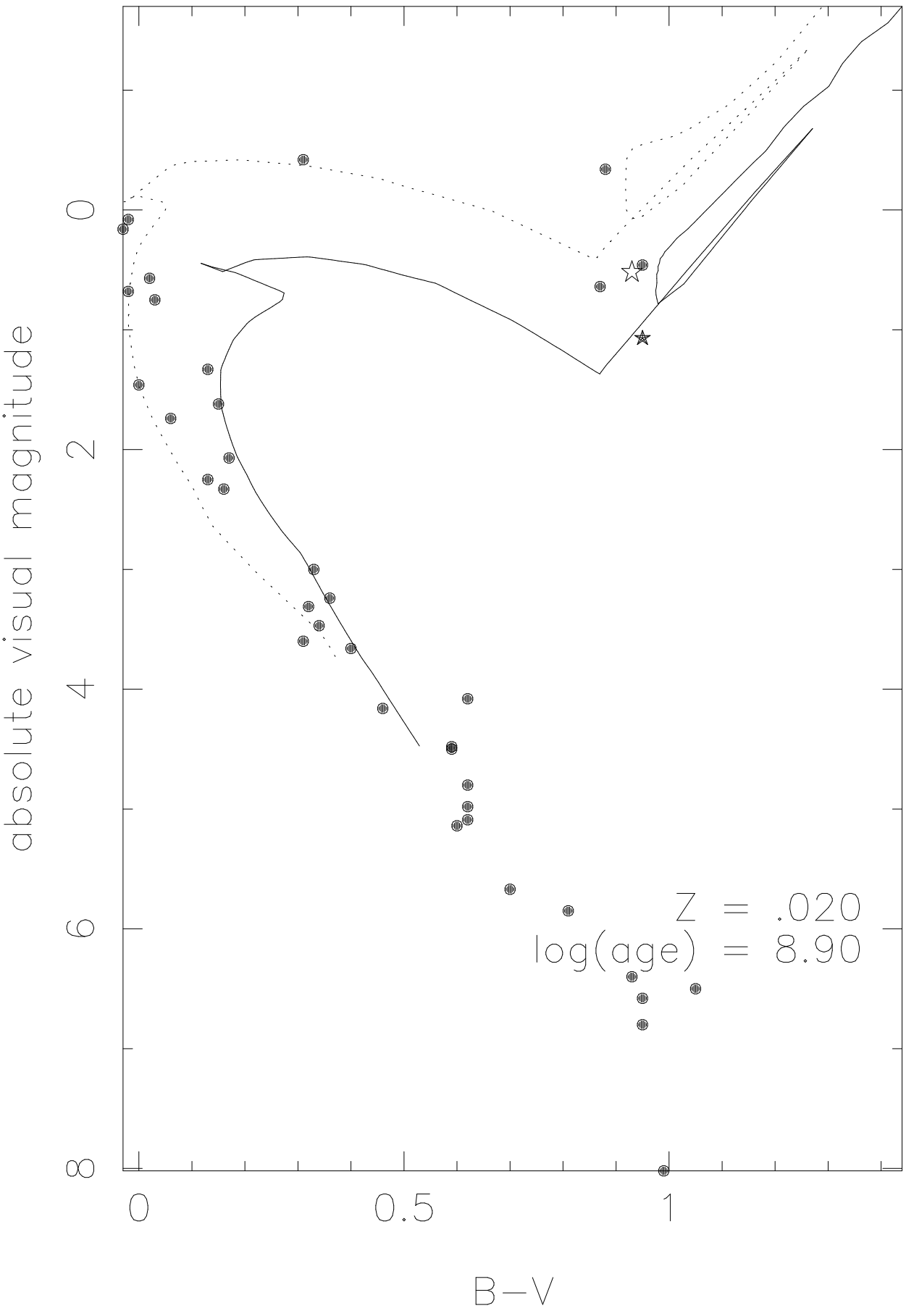

Fig. 5.— Color-magnitude diagram for η Andromedae (open and filled star symbols denoting primary and secondary component, respectively) and members of the Ursa Major stream

Table 1: Spectroscopic elements (Gordon 1946)

e	0.005±0.047
ω	$166\overset{\circ}{.}4 \pm 104\overset{\circ}{.}3$
T	JD 2430119.1 ± 32.5 days
P	115.71 days
K_1	17.89±0.65 km/s
K_2	19.83±1.01 km/s

Table 2: Orbital and system elements
from the Mark III interferometer

Parameter	value	formal uncertainty[a]	range[b]
a/mas	10.37	0.03	10.33–10.40
e	0.006	0.002	0.004–0.008
i	$30\overset{\circ}{.}5$	$0\overset{\circ}{.}4$	30.1–30.9
Ω	$69\overset{\circ}{.}4$	$0\overset{\circ}{.}5$	68.8–70.0
ω	215°	4°	213°–222°
T	JD2448013	1	2448012 – 2448015
P/days	115.72	0.01	115.70–115.74
D_1/mas (800 nm)	1.4	0.1	1.2–1.6
D_2/mas (800 nm)	1.0	0.3	0.6–1.4
$\Delta m_{800\mathrm{nm}}$	$0\overset{\mathrm{m}}{.}50$	$0\overset{\mathrm{m}}{.}04$	$0\overset{\mathrm{m}}{.}45 - 0\overset{\mathrm{m}}{.}55$
$\Delta m_{550\mathrm{nm}}$	$0\overset{\mathrm{m}}{.}55$	$0\overset{\mathrm{m}}{.}06$	$0\overset{\mathrm{m}}{.}46 - 0\overset{\mathrm{m}}{.}61$
$\Delta m_{500\mathrm{nm}}$	$0\overset{\mathrm{m}}{.}56$	$0\overset{\mathrm{m}}{.}07$	$0\overset{\mathrm{m}}{.}45 - 0\overset{\mathrm{m}}{.}63$

[a] from matrix inversion

[b] from Monte Carlo simulation (see Sect. 4)

Table 3. Observation and result log for η Andromedae

UT Date (1)	Bess. Yr. (-1900) (2)	BL [m] (3)	No. scans (4)	ρ [mas] (5)	θ [deg] (6)	$\sigma_{\rm maj}$ [mas] (7)	$\sigma_{\rm min}$ [mas] (8)	φ [deg] (9)	O-C [mas] (10)
1990									
Jul 15	90.5359	27.6	3	9.01	157.15	0.57	0.04	107.1	0.09
Jul 27	90.5687	31.5	13	9.48	199.66	0.12	0.02	105.8	0.08
Jul 29	90.5742	27.0	9	9.64	207.87	0.17	0.02	105.2	0.39
Aug 12	90.6125	23.6	10	9.99	243.75	0.43	0.05	102.7	0.48
Aug 17	90.6262	27.6	16	10.08	258.93	0.12	0.03	98.5	0.19
Aug 23	90.6426	31.5	13	10.00	276.24	0.09	0.02	96.9	0.04
Aug 28	90.6563	27.0	19	9.62	291.26	0.08	0.02	93.3	0.03
Aug 29	90.6591	23.3	16	9.67	293.98	0.06	0.01	85.7	0.17
Aug 31	90.6646	23.3	11	9.41	300.49	0.24	0.02	81.0	0.08
Sep 1	90.6673	19.4	25	9.30	304.30	0.06	0.02	82.2	0.02
Sep 3	90.6728	15.4	14	9.09	311.80	0.09	0.03	100.6	0.14
Sep 7	90.6837	15.2	10	8.80	327.23	0.61	0.09	78.9	0.37
Sep 15	90.7056	15.4	23	8.99	353.63	0.08	0.02	92.4	0.06
Oct 28	90.8233	31.5	15	9.50	120.63	0.08	0.02	98.0	0.04
1991									
Aug 9	91.6037	27.0	9	9.50	287.68	0.22	0.04	105.1	0.18
Aug 28	91.6557	31.5	13	8.97	353.63	0.10	0.02	88.5	0.04
Aug 29	91.6584	23.6	15	9.00	356.84	0.12	0.03	98.1	0.03
Sep 16	91.7077	23.6	15	10.27	53.13	0.10	0.03	96.5	0.02
Sep 17	91.7104	23.6	14	10.22	55.39	0.08	0.02	99.7	0.11
Sep 18	91.7132	27.0	16	10.32	58.35	0.05	0.01	84.4	0.03
Sep 30	91.7460	12.0	18	10.01	90.65	0.08	0.02	84.3	0.19
1992									
Aug 22	92.6413	23.1	15	9.91	36.15	0.19	0.03	85.5	0.11
Aug 23	92.6441	23.1	10	10.27	40.55	0.56	0.05	96.3	0.49

Table 4: Diameters and magnitudes

	Band, effective wavelength [nm]		
	$I_{\rm C}$	V	B
	800	550	450[a]
D_1	1.4 mas	1.3[b]	1.3[b]
D_2	1.0 mas	0.9[b]	0.9[b]
M_1	$-0\overset{\rm m}{.}40 \pm 0\overset{\rm m}{.}06$	$0\overset{\rm m}{.}52 \pm 0\overset{\rm m}{.}06$	$1\overset{\rm m}{.}45 \pm 0\overset{\rm m}{.}06$
M_2	$0\overset{\rm m}{.}10 \pm 0\overset{\rm m}{.}07$	$1\overset{\rm m}{.}07 \pm 0\overset{\rm m}{.}07$	$2\overset{\rm m}{.}02 \pm 0\overset{\rm m}{.}08$
m^c_{1+2}	$3\overset{\rm m}{.}48$	$4\overset{\rm m}{.}42$	$5\overset{\rm m}{.}36$

[a] Extrapolated from 500 nm (see text)

[b] Adopted (diameters are for uniform disks)

[c] Johnson *et al.* 1966